Thermally Bonded Nonwoven Filters Composed of Bi-Component Polypropylene/Polyester Fiber. II. Relationships between Fabric Area Density, Air Permeability, and Pore Size Distribution

X. Y. Wang, R. H. Gong

Textiles and Paper, School of Materials, The University of Manchester, Manchester, United Kingdom

Received 21 September 2005; accepted 26 January 2006
DOI 10.1002/app.24169
Published online in Wiley InterScience (www.interscience.wiley.com).

ABSTRACT: The relationships between the pore size, fabric area density, and air permeability of the three-dimensional (3D) nonwoven filter samples produced using a new 3D forming process has been studied. Results indicate that the thermally bonded nonwoven filter samples consist of multiple filtration layers of interconnected pores and tortuous pore paths through the fabric thickness. Both the bubble point pore diameter and the mean flow pore diameter of the produced filter samples increase linearly with increase in the reciprocal of the fabric area density. The air permeability of the nonwoven filter samples decreases significantly to a certain value with increasing fabric area density, and then becomes almost stable with further increasing of fabric area density. The measured pore size data in the thermally bonded nonwoven samples were found to follow all the bi-normal, bi-lognormal, and bi-Weibull distributions. Taken into account together the pore structure, pore size distribution, air permeability, and fabric area density, the new 3D forming system can substitute most of the commercial polyester filter media with significantly reduced costs.
 J Appl Polym Sci 102: 2264–2275, 2006

Key words: fibers; processing; structure; filtration; statistical analysis

INTRODUCTION

Three kinds of pores may be present in a material; closed, blind, and through pores. The closed pores are not accessible. The blind pores terminate inside the material and do not permit fluid flow. The through pores are open to the outside and permit fluid to flow. Pore structure characteristics of nonwovens are important for their applications.[1,2] Through pores are of primary interest for many of the applications of nonwovens, such as fluid barriers and filter media.[1,2] Important characteristics of through pores in nonwovens include the pore size, such as the bubble point pore diameter and the mean flow pore diameter, pore size distribution, and air permeability.

The performance of filter media is influenced by both the pore size and pore size distribution within the media materials. During the filtration processing, the pore size, pore size variation, and the accessibility of pore to the passage of air or other fluids are very important. Although it is logical to expect that the air permeability of nonwovens is dependent on the pore size, and the pore size is dependent on the constituent fibers and the fabric area density, there is limited experimental evidence of an attempt to correlate these parameters in the literature.[2] Recently, Epps and Leonas[2] investigated the relationship between the pore size and the air permeability of the spunlaced and spun/meltblown/spunbonded (SMS) fabrics. They reported that there was a significant correlation between the air permeability and the pore size, characterized using both the bubble point pore diameter and the mean flow pore diameter for the SMS fabrics. For the spunlaced fabrics, the air permeability had negative correlation with the mean flow pore size. There is little information available in the literature on the relationships between the pore size, fabric area density (fabric weight), and the air permeability for thermally bonded nonwovens.

In the other limited studies[3–5] that addressed the relationship between the air permeability and structural characteristic of nonwovens, including fabric weight, thickness, and fiber diameter, the nonwovens were needle punched. These studies have shown that air permeability decreases nonlinearly as thickness and fabric weight increases, and the fabric weight had a more significant influence on air permeability than either thickness or fiber size.[3]

In the first part of the present study,[6] the pore structures of the three-dimensional (3D) nonwoven

Correspondence to: X. Y. Wang (ljfwxy@yahoo.com).
Contract grant sponsor: The Department of Trade and Industry (UK); contract grant number: KBBB/C/012/00028.

filter samples, produced using a new 3D forming process based on air laying and through-air thermal bonding were characterized using capillary flow porometer. A statistical approach, involving statistical experiment design and regression analysis, was used to minimize the bubble point pore diameter and mean flow pore diameter, and obtain the optimized thermal bonding process parameters. In this paper, the effects of constituent fibers and the fabric weight (area density) on the bubble point pore diameter and mean flow pore diameter were further investigated. The objective of this paper is to explore the relationships between the pore size, fabric area density, and air permeability of the nonwoven filter samples produced using the presently developed thermally bonding process.

The air permeability is associated with the pore size and also with the pore size variation. Thus, it is also necessary to investigate the pore size distribution. However, the reported results of pore size for the nonwoven fabrics were generally given only as one value or the mean of finite values, and little attention was paid to the statistical characteristics of the pore size variations in the literatures.[1,2] Thus, another important objective of this study is to statistically analyze the measured data of the pore diameters of both the nonwoven samples and commercially available filter products. The related statistical characteristics between the former and the latter were compared to evaluate the quality of the nonwoven filter samples made using the new 3D system.

EXPERIMENTAL

The newly developed 3D forming process is based on air laying and through-air thermal bonding. The nonwoven filter samples, with different area density, were prepared using the optimized thermal bonding process parameters reported previously.[6] These are thermal bonding temperature of 159°C, dwell time of 6 s, and hot air velocity of 3.4 m/s. The area density, i.e., the fabric weight per unit area, was measured by weighing the samples with an area of 50×50 mm^2 using a balance with an accuracy of 0.001 g. To investigate the effects of the constituent fibers, in addition to the polypropylene (PP)/polyester (PET) (sheath/core) bi-component fiber, a mixture of 90% PP/PET bi-component fiber and 10% PP fiber was also used to produce the thermally bonded nonwoven filter samples.

Air permeability is the rate of air flow passing perpendicularly through a known area fabric under a differential pressure between two fabric surfaces.[7] Air permeability measurements were also carried out using the completely automated capillary flow porometer, model CFP 1500 AEX manufactured by PMI, as detailed previously.[6] The nonwoven filter samples were cut into circular samples of 75 mm in diameter for the measurement.[7] Prior to the tests, the samples were conditioned in the standard atmosphere for testing textiles, i.e., a relative humidity of 65% ± 2% and a temperature of 20 °C ± 2°C for 24 h.[8] The direct result for the air permeability measurement was recorded as the relationship between the differential gas pressures and the gas flow rates. The air permeability was obtainable at any desired pressure from flow rates of any nonreacting gas measured as a function of pressure. In the present study, the air permeability corresponding to the differential pressure of 20 mm H_2O was taken for the comparisons between the different samples.

For the measurements of pore parameters, the samples were soaked in silicon oil that filled the pores of the samples, also following the conditioning in the standard atmosphere for testing textiles. Such samples are referred to as wet samples. It is crucial to make sure that all the pores in the wet sample were filled with the silicon oil that does not interact with the samples. As mentioned previously,[6] the pore diameter is calculated from differential pressure by applying eq. (1) to the average pressure–flow response of three repeats.

$$D = 4C\gamma/P \tag{1}$$

where D is the pore diameter, γ is the surface tension of the liquid, P is the differential pressure, and C is a constant (2860 when P is in Pa and 0.415 when P is in psi).

Equation (1) shows that the differential pressure required to displace the liquid in a pore is inversely proportional to the pore diameter. Therefore, the pressure differential required to displace the liquid in a pore would be the highest at the most constricted part of the pore. Once the highest pressure is reached, the liquid from the rest of the pore will be removed, and the gas will start flowing through the pore so that the presence of the pore can be detected. Obviously, the pore diameters determined by such an extrusion flow porometry are the constricted pore diameters.

The largest pore opens up at the lowest pressure, the bubble point pressure, at which the flow starts through the wet sample. The pore diameter calculated from this pressure is the largest pore diameter or termed as the bubble point pore diameter. From the mean flow pressure at which the amount of flow that passes through a wet sample is half the flow that passes through a dry sample, the mean flow pore diameter can be determined. Both the bubble point pore diameter and the mean flow pore diameter are important characteristics reflecting the pore size and flow properties of a nonwoven filter sample. By comparing the gas flow rate of a wet sample and that of a corresponding dry sample at the same pressure, the percentage of flow passing through the pores larger

than or equal to a specified size can be calculated from the pressure–size relationship. By increasing pressure in small steps, the flow contribution of very small pore size increments can be determined. Then the pore distribution can be described as the distribution function, f:

$$f = -\frac{d(F_w/F_d)}{dD} \times 100 \tag{2}$$

where F_w and F_d are flow rates through wet and dry samples, respectively, at the same differential pressure and D is pore diameter.[1]

In addition to the evaluation of pore structures, the surface morphologies and the cross-sectional structures of the nonwoven filter fabrics were also observed using SM-300 scanning electron microscope (SEM).

STATISTICAL ANALYSIS

For statistical analysis of the measured data of the pore diameters, the normal, lognormal, and Weibull distributions that are widely used to fit experimental data were used and compared. The theoretical normal, lognormal, and Weibull distributions[9–13] can be expressed as eqs. (3)–(5), respectively:

$$f(x) = \int \frac{1}{\sigma\sqrt{2\pi}} \exp -\frac{(x-\mu)^2}{2\sigma^2}\, dx \tag{3}$$

$$f(\ln x) = \int \frac{1}{\sigma_{\ln}\sqrt{2\pi}} \exp -\frac{(\ln x - \mu_{\ln})^2}{2\sigma_{\ln}^2} d\ln x \tag{4}$$

$$f(x) = 1 - \exp -\left(\frac{x}{x_0}\right)^m \tag{5}$$

where $f(x)$ or $f(\ln x)$ is the cumulative probability, x is the pore size (here, the pore radius) data, μ and σ are the mean and standard deviation of series x, $\mu_{\ln}$, and $\sigma_{\ln}$ are the mean and standard deviation of logarithms of series x, x_0 is the scale parameter, below which 63.2% of the data lie, of Weibull distribution and m is the Weibull modulus which reflects the data scatter within the distribution. Thus the cumulative probability curve will show approximate pattern of linearity on the normal probability coordinate, lognormal probability coordinate, and Weibull probability coordinate if a data set follows the normal, lognormal, and Weibull distribution, respectively. For lognormal distribution, it can also use the normal probability coordinate if the data x are transformed into the logarithm $\ln x$. The validity of the assessments can be judged by the correlation coefficient γ between x and $f(x)$:[13]

$$\gamma = \frac{1}{n}\sum_{i=1}^{n}\left(\frac{x_i - \mu}{\sigma}\right)\left(\frac{f(x_i) - \overline{f(x)}}{\sigma_{f(x)}}\right) \tag{6}$$

where $\overline{f(x)}$ and $\sigma_{f(x)}$ are the mean and standard variation of the expected theoretical distribution $f(x)$. The closer to 1 the correlation coefficient, the more confidently the expected theoretical distribution describes the measured results. Further details of calculation of mean, standard variation, the scale parameter, and Weibull modulus can be found elsewhere.[12–14] A Weibull plot can be drawn by rearranging eq. (4) and taking natural logarithms twice, i.e.,

$$\ln\left[\ln\frac{1}{1-f(x)}\right] = m(\ln x - \ln x_0) \tag{7}$$

Therefore, the desired Weibull parameters, x_0 and m, can be determined by fitting eq. (7).[14,15]

In addition, coefficient of correlation (COC) can be used to evaluate the relationship between two variables in the light of linear term.[16] The COC between two variables, x_i ($i = 1, 2, \ldots, n$) and y_i ($i = 1, 2, \ldots, n$), is defined as:

$$R(x,y) = \frac{\sum_{i=1}^{n}\left(x_i - \frac{1}{n}\sum_{j=1}^{n} x_j\right)\left(y_i - \frac{1}{n}\sum_{j=1}^{n} y_j\right)}{\sqrt{\sum_{i=1}^{n}\left(x_i - \frac{1}{n}\sum_{j=1}^{n} x_j\right)^2}\sqrt{\sum_{i=1}^{n}\left(y_i - \frac{1}{n}\sum_{j=1}^{n} y_j\right)^2}} \tag{8}$$

The closer the absolute of the COC R is to 1, the more significant is the relationship between the two variables in the light of linear term. It should be stated that a low COC R only means a weak linear relationship between two variables, and do not deny other possible relationship existing between the variables.

RESULTS AND DISCUSSION

Structure characteristics of the nonwoven filter samples

Figure 1 presents the SEM images of the surface morphologies of the thermally bonded nonwoven fabrics using the two types of fibers, PP/PET bi-component fiber and a mixture of 90% PP/PET bi-component fiber and 10% PP fiber. It can be seen that fibers were dispersed randomly to form irregularly shaped pores with a large variation in size within both the nonwoven fabrics. There appeared molten PP fibers that were distributed on the web in the form of segments in the nonwoven fabric consisting of the mixture of the PP/PET and PP fibers. Figure 2 shows the correspond-

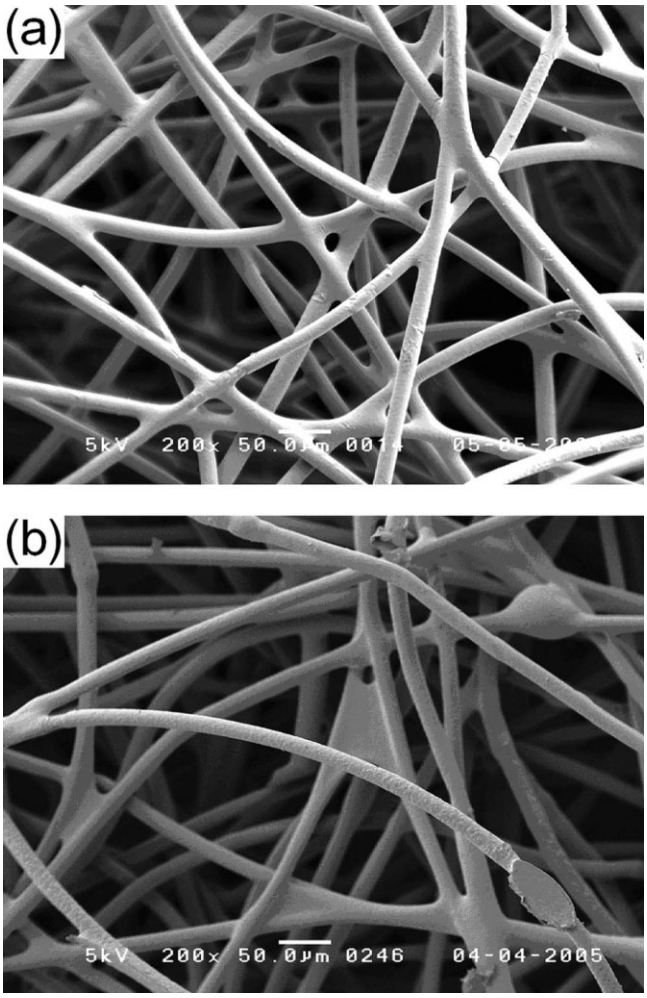

Figure 1 SEM images showing the surface morphologies typical of the thermally bonded nonwoven fabrics produced using (a) PP/PET bi-component fiber and (b) 90% PP/PET bi-component fiber and 10% PP fiber.

ing cross-sectional structures of the above two nonwoven fabrics. There exist multiple fiber ends through the thickness, which indicates that multiple filtration layers were formed by randomly dispersed fibers. These are similar to the multiple filtration layers within the stainless steel fiber web prepared by Li.[17] Generally speaking, the nonwoven samples made from shorter fibers with smaller diameters have multiple filtration layers with interconnected pores and tortuous pore paths through the fabric thickness.[17]

Figure 2 also reveals that the inner layers closer to the mold surface are denser than the outsider layers of the nonwoven fabrics. This could be attributed to the stress gradient existing in the thickness direction of fabrics during the thermal bonding process. The hot air used for the bonding impacted the formed webs and caused stress gradient within the web. Because of the direct action of the mold surface on the web, there were relatively higher compressed stresses within the inner layer than those within the outside layers of the bonded webs, leading to much denser inner layers than the outside layers. Such a structure is very helpful in the filtration process. The more porous part could be placed towards upstream to obtain greater capacity of absorbing particles from the feed stream, while the denser part could trap the smaller particles.

During the filtration process, the solid particles are rigid and un-deformable under the filtration condition. When they pass through the thermally bonded nonwoven filter media, the particles that could be trapped are influenced by the filter medium structure. As mentioned earlier, there are multiple layers with interconnected pores and pore paths are tortuous in the thermally bonded nonwoven fabrics. During filtration, the particles can be trapped by pores in any one of the multiple filtration layers. Where there is a trapped particle, the pore size would be decreased. The pores with decreased size will trap particles more efficiently. Unlike isolated pores that could be plugged up easily, the interconnection among the

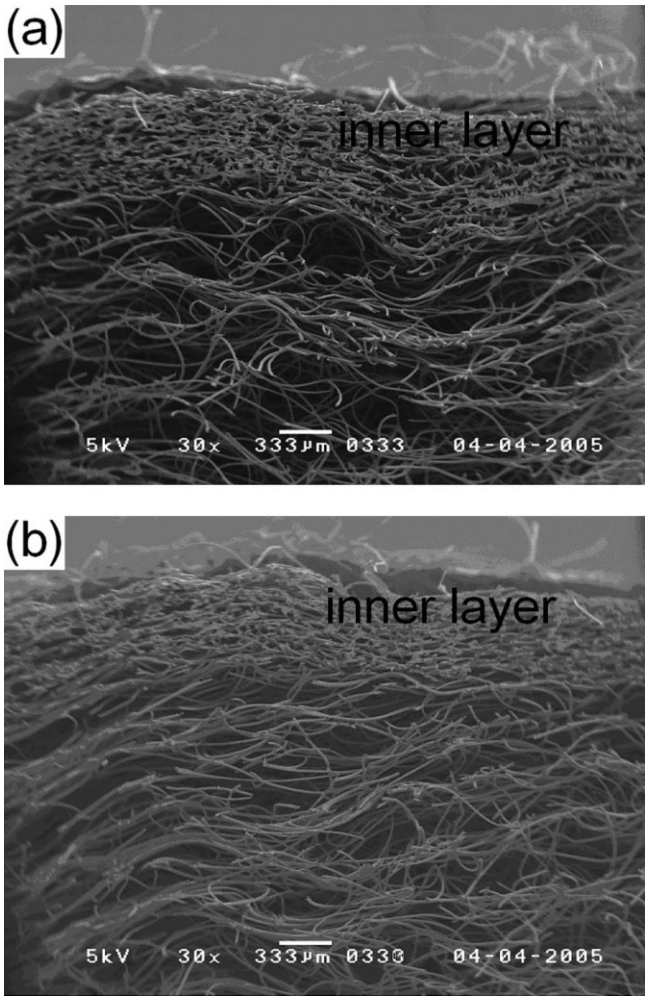

Figure 2 SEM images showing the cross-sectional structures typical of the thermally bonded nonwoven fabrics produced using (a) PP/PET bi-component fiber and (b) 90% PP/PET bi-component fiber and 10% PP fiber.

pores and high porosity of the thermally bonded nonwoven fiber media would prevent the pores from clogging, and hence, result in higher filtration efficiency.

As for the filtration capacity, the thermally bonded nonwoven media also have the following useful structural characteristics: high porosity, large density gradient, and the multiple filtration layers structure. These would result in extended time to reach a given pressure drop resulting from the decrease of the air permeability. Large particles have a high probability of being stopped in the top filtration layers or in the layers with less density, and smaller particles will more likely be trapped in subsequent inner and denser layers. The interconnection among pores can prevent the nonwoven media from being clogged easily at locations where there are trapped particles. As a result, it will take a longer time to blind the media. The pressure drop would increase as a result of a decrease of the permeability resulting from the trapping of particles in filter media. The structural characteristics of the thermally bonded nonwoven filter samples can also result in a large dirty holding capacity and a slow increase of pressure drop with increase in time. These arguments may expect a longer filter life, fewer filter changeovers, and less downtime from the thermally bonded nonwoven filters, despite the fact that the comparison data with the commercial filters are not available so far.

Effects of fabric area density and constituent fibers

Figures 3 and 4 present the plots of the bubble point pore diameter and the mean flow pore diameter versus the fabric area density respectively. Li[17] pointed out that the number of filtration layers in a filter medium is determined by the size and density of fibers, their dispersion, and the basis weight and porosity of the medium. The number of filtration layers N in a filter medium can be estimated as follows:[17]

$$N = k\int \frac{t_i}{d_i} - 1 \tag{9}$$

where k is a structural or geometric factor, $k \leq 1$, depending on the fiber dispersion and packing density (porosity), and t_i is the thickness of the layer consisting of fibers with an average diameter d_i. The maximum number of filtration layers N_{max} can be predicted with $k = 1$. Generally, the bigger the fabric area density is and the thicker the fabric is, the more filter layers it contains. This can explain why both the bubble point pore diameter and the mean flow pore diameter decrease as the fabric area density increases, as shown in Figures 3 and 4.

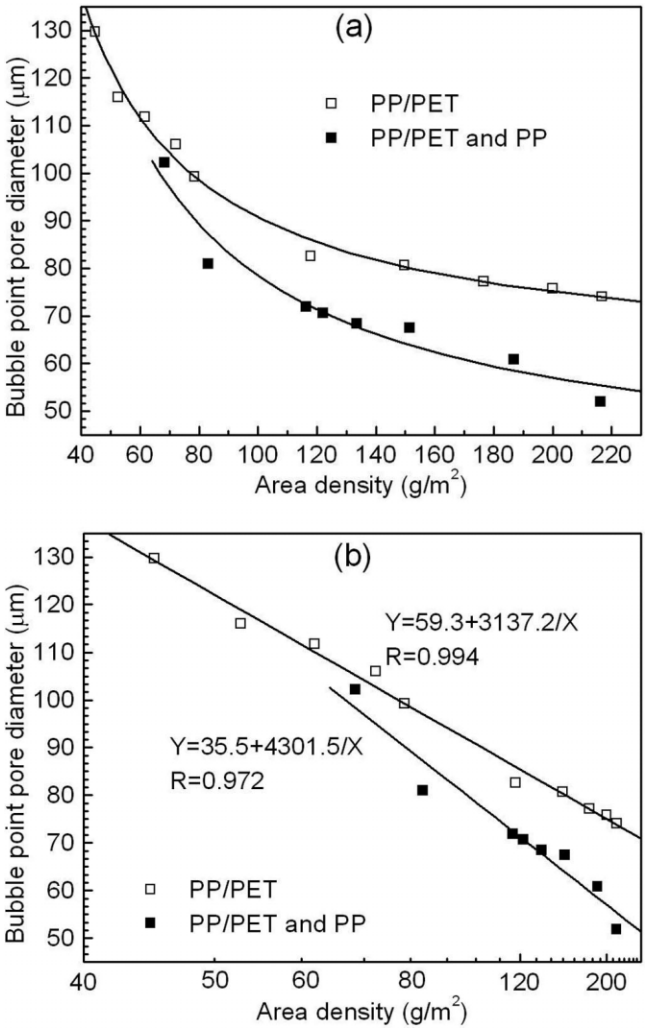

Figure 3 Bubble point pore diameter with respect to the fabric area density for the thermally bonded nonwoven filter samples. (a) Linear–linear coordinates; (b) reciprocal–linear coordinates. Note that X and Y in the fitted equations stand for the area density and the bubble point pore diameter respectively; R values are the coefficients of correlation.

From Figures 3 and 4, it can be also seen that the nonwoven samples produced using the mixture of 90% PP/PET and 10% PP fibers have both smaller bubble point pore diameters and smaller mean flow pore diameters than the nonwoven samples produced using the PP/PET fiber. This can be attributed to the different bonding structures as shown in Figure 1. There appeared the molten PP fibers that were distributed on the web in the form of segments in the thermally bonded nonwoven fabrics produced using the mixture of 90% PP/PET and 10% PP fibers. This can be further ascribed to the fact that the PP fibers were completely molten during the thermal bonding processing, leading to groups or clusters distributed on the fiber web, and hence the formation of the segmented bonding structure. Consequently, the thermally bonded nonwoven fabrics constituting both PP/

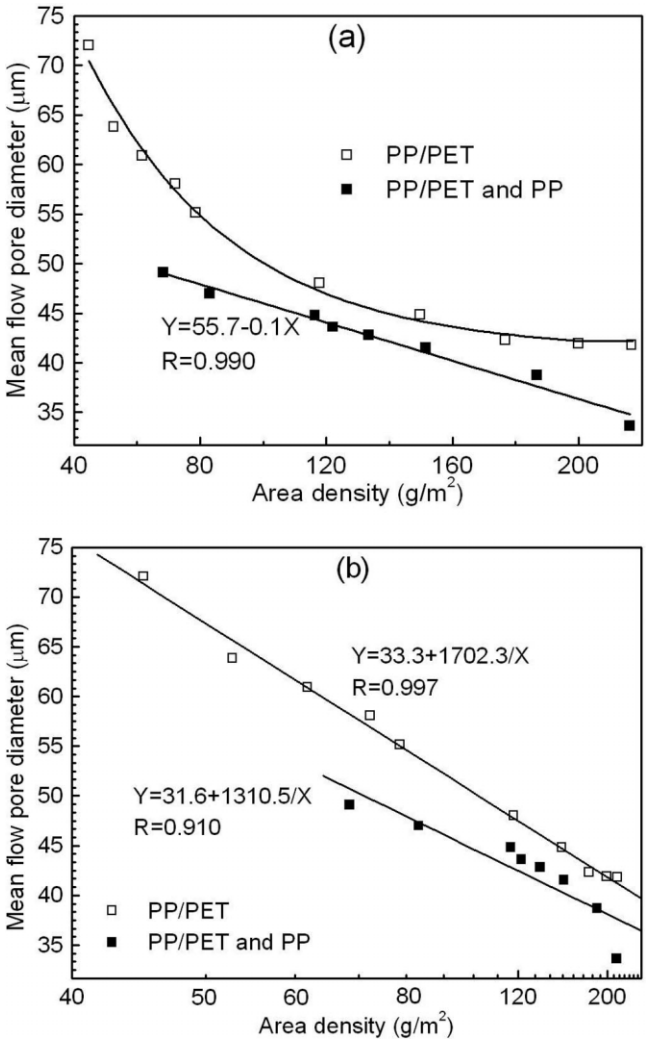

Figure 4 Mean flow pore diameter with respect to the fabric area density for the thermally bonded nonwoven filter samples. (a) Linear–linear coordinates; (b) reciprocal–linear coordinates. Note that *X* and *Y* in the fitted equations stand for the area density and the mean flow pore diameter respectively; *R* values are the coefficients of correlation.

PET and PP fibers have smaller bubble point pore diameters and mean flow pore diameters than the corresponding fabrics consisting of only PP/PET bi-component fiber.

Furthermore, Figures 3 and 4 show that the bubble point pore diameters of both the PP/PET and PP/PET + PP samples decrease nonlinearly with increase in the fabric area density, and linearly with the reciprocal fabric area density. However, mean flow pore diameters of the two kinds of samples behave differently. The mean flow pore diameter of the PP/PET samples decreases nonlinearly with the fabric area density, and linearly with the reciprocal fabric area density, the same as their bubble point pore diameter. On the other hand, the mean flow pore diameter of the PP/PET + PP samples follows a linear relationship that is lost when reciprocal linear coordinates are used, with their fabric area density. Such results are probably associated with the high porosity, interconnected pores, and tortuous pore paths through the thermally bonded nonwoven fabric thickness. Consequently, the silicon oil, used as the liquid to measure the pore size, has a low viscosity and can easily twist and turn on entering and leaving an individual filtration layer in searching for the passages through multiple layers in the filter media. Obviously, the larger is the pore, the more severe is the effect of the twisting and turning on entering and leaving an individual filtration layer on the measured pore sizes. Such effect was hence significant for the relatively larger mean flow pore diameter of the PP/PET samples and the bubble point pore diameters of both the PP/PET and PP/PET + PP samples, but negligible for the relatively smaller mean flow pore diameter of the PP/PET + PP samples. This is probably the reason why the curves of the mean flow pore diameter of the PP/PET + PP samples behave differently from the other curves shown in Figures 3 and 4.

Relationships between pore size, fabric area density, and air permeability

Figure 5 presents the air flow rate with respect to differential pressure for the nonwoven filter samples produced using the bi-component PP/PET fiber and with different fabric area densities. Clearly, there exists a nonlinear relationship between the air flow rate and the differential pressure. Hassenboehler[18] made use of air permeability measurements over a range of pressure drop in analyzing fabric pore structure. He proposed that the changes in the slope of the pressure drop–permeability curve mark the onset of nonlinear

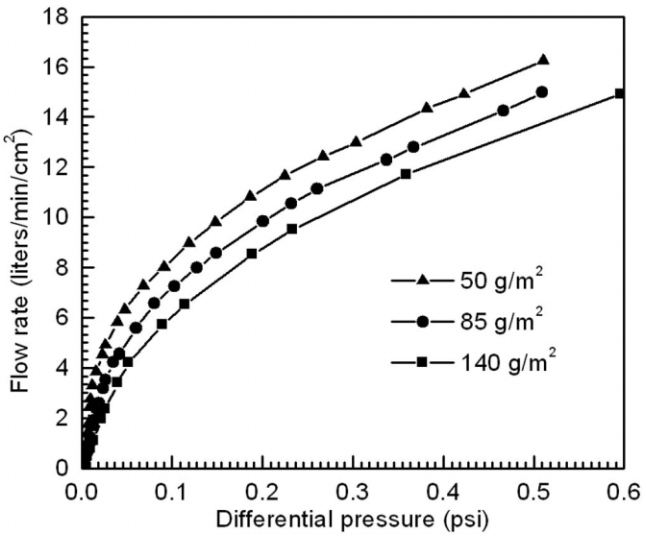

Figure 5 The air flow rate with respect to differential pressure for the thermally bonded nonwoven filters.

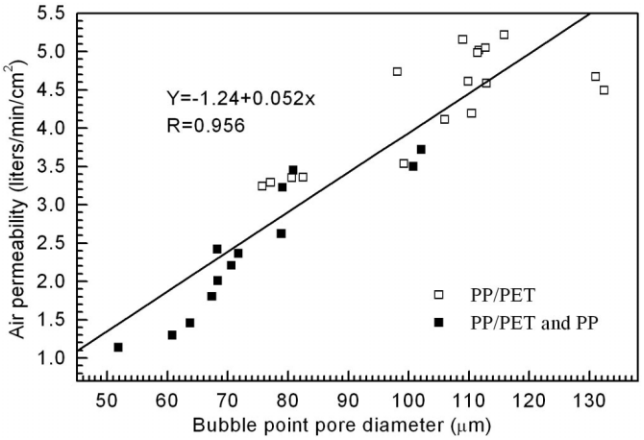

Figure 6 Plot of air permeability versus bubble point pore diameter for the thermally bonded nonwoven filter samples (*R* is the coefficient of correlation, the differential pressure used is 20 mm H_2O).

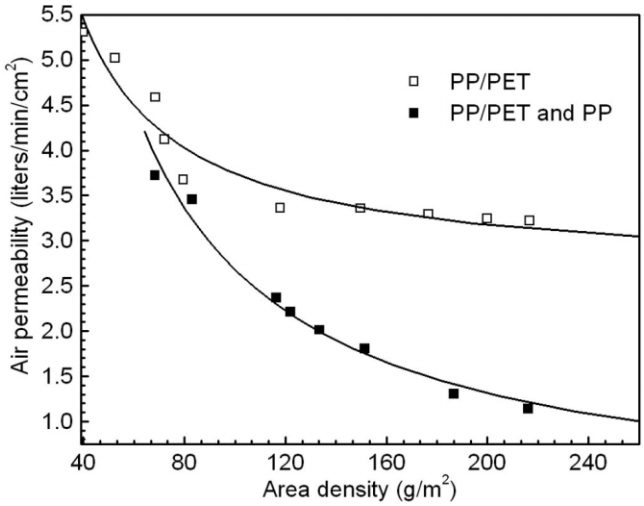

Figure 8 Plot of air permeability versus fabric area density for the thermally bonded nonwoven filter samples.

air flow, turbulence in the initial flow channels, and the addition of discrete air flow in separate, smaller channels. As the differential pressure is gradually increased, air flow is initiated through successively smaller pores. Previous work[19] demonstrated that there is a nonlinear relationship between air permeability measurements and the differential pressure at which the test is performed for the various fabrics, such as the screen fabrics. This is very similar to the present result as shown in Figure 5.

Figures 6 and 7 present the plots of the air permeability versus the bubble point pore diameter and the mean flow pore diameter respectively, for the thermally bonded nonwoven filters with the different fabric area densities. In both figures, the data for the filter samples produced using the PP/PET fiber and using the mixture of the PP/PET and PP fibers have been merged together. An increasing trend of the air permeability with increasing the pore diameter can be detected. This shows that in a statistical sense the air flow increases as both pore sizes increase.

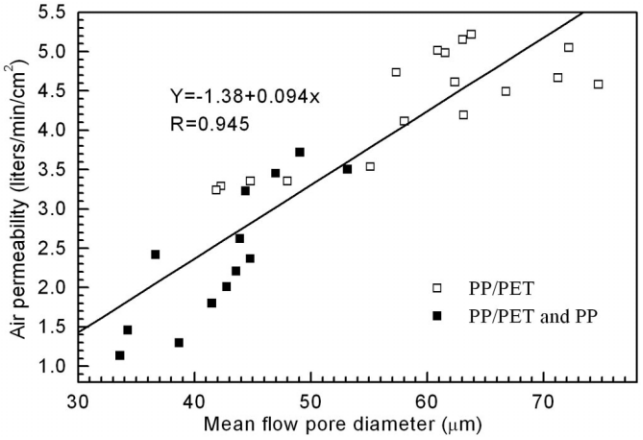

Figure 7 Plot of air permeability versus mean flow pore diameter for the thermally bonded nonwoven filter samples (*R* is the coefficient of correlation, the differential pressure used is 20 mm H_2O).

The above results are in an agreement with those of Epps and Leonas[2] for spunbonded/meltblown/spunbonded (SMS) fabrics. They reported that for the SMS fabrics, there is a significant linear correlation between the air permeability and both the bubble point pore diameter and the mean flow pore diameter. However, there exists a negative linear correlation between the air permeability and the mean flow pore diameter for the spunlaced fabrics, but no clear correlation between the air permeability and the bubble point pore diameter. This may be due to the difference in fabric structure between the spunlaced fabrics and the present thermally bonded nonwoven filter samples. The spunlaced fabrics are manufactured employing jets of water to entangle fibers, and rely primarily on fiber-to-fiber friction to achieve physical integrity. Thus, the entangled structures are more compressible than thermally bonded ones, as well as having mobility and partial alignment of fibers in the thickness direction. When subject to air pressure, individual fibers can migrate more easily within the spunlaced fabrics than within the thermally bonded fabrics. This should be accountable for the different relationships between the air permeability and the bubble point pore diameter for the two types of nonwoven fabrics. However, it is not clear why there exists a negative linear correlation between the air permeability and the mean flow pore diameter for the spunlaced fabrics.

Figure 8 presents the plots of air permeability versus fabric area density for the thermally bonded nonwoven filter samples. It is observed that the air permeability decreases nonlinearly as the fabric area density increases: it decreases significantly to a certain

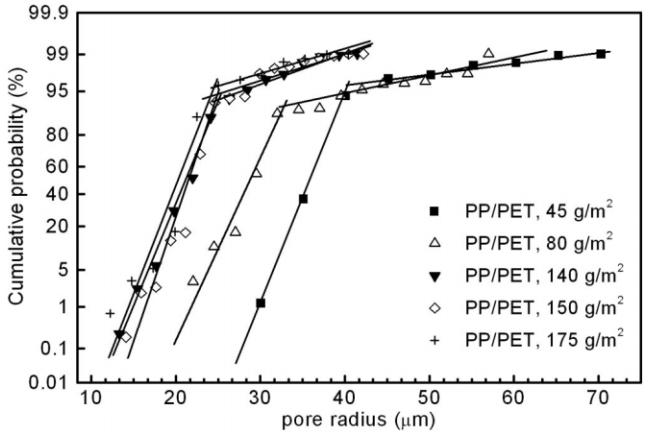

Figure 9 The cumulative probability curves of pore radius data series for samples with different fabric area densities on normal probability coordinates.

value with increasing fabric area density, and then it becomes almost stable with further increase in the fabric area density. Such a result may due to the effects of the high porosity and a density gradient structure with interconnected pores and tortuous pore paths through the fabric thickness. As shown in Figure 2, the inner layer is obviously denser and transited to the porous outer layer for the density gradient structure of the filter samples. When the fabric area density increases slightly, for a lighter fabric area density, i.e., a thinner thickness, the additional layer is relatively denser than that for a heavier fabric density, i.e., a thicker thickness. Consequently, the former additional layer leads to a more significant decrease in the air permeability than the latter additional layer. Furthermore, when the fabric area density increases up to a certain value, the additional layers are all highly porous and have approximately same resistance to air flow. These should be the reasons for the observed nonlinear relationship between the air permeability and the fabric area density.

Statistical analysis of pore size variation

All the cumulative probability curves of pore radius or the logarithm of pore radius for the thermally bonded nonwoven samples on the normal probability coordinates and Weibull probability coordinates show the approximate patterns of bi-model linearity, i.e., the data series for all samples can be fitted very well as two linear segments. Figure 9 gives the cumulative probability curves of pore radius for some thermally bonded nonwoven samples on the normal probability coordinates. Therefore, it can be concluded that the pore size variations in the thermally bonded nonwoven samples follow all the bi-normal, bi-lognormal, and bi-Weibull distributions. Accordingly, these experimental pore size series for each sample can be described using two sets of characteristic parameters, each set for one of the two linear segments, rather than one set of characteristic parameters for the normal, lognormal, and Weibull distributions as expressed by eqs.(3)–(5). However, it cannot be determined which distribution is the most suitable to describe the pore size variations, which is also impossible to be judged through further statistical analysis and test. It is possible that a data set follows one theoretical distribution at a certain level, but it may belong to another theoretical distribution.[12]

Sampson and coworkers[20–23] studied the pore radius distribution in near-planar stochastic fiber networks, such as paper and glass fiber filter mats. They found that the pore radius variations in these fiber networks can be well described by the lognormal or γ distributions. This was somewhat different from the present result. The statistical analysis shows that the pore size variations in the thermally bonded nonwoven samples seem to follow all the bi-normal, bi-lognormal, and bi-Weibull distributions.

Since all the three bi-model models can well describe the pore size variations in the thermally bonded nonwoven samples, the characteristic parameters in any one of these distributions can be used for comparison among the different samples. In the present study, four characteristic parameters in the bi-normal distribution, as shown in Figure 10, have been used. Here r_T and P_T are the pore radius and cumulative probability at the intersect point of the two fitted lines, and r_S and r_L are the pore radii corresponding to the medians of the cumulative probability on the two fitted linear segments at the smaller and larger pore radii, respectively. Obviously, the four characteristic

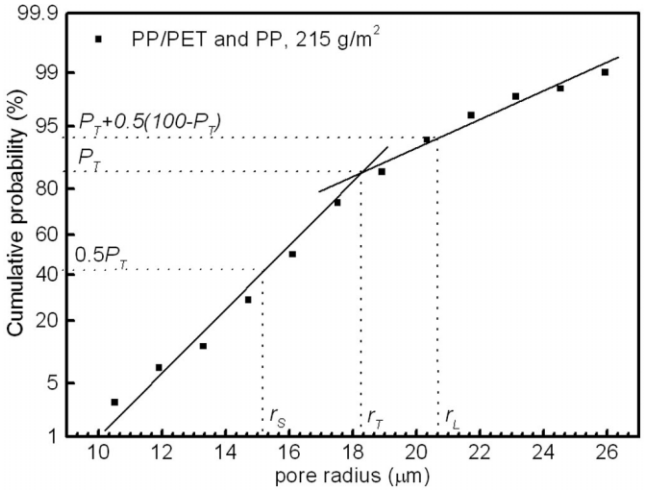

Figure 10 The plot of bi-normal distribution of pore radius data series for one sample with the fabric area density of 215 g/m^2 produced using the mixture of PE/PET and PE fibers (for illustrating the calculation of the characteristic parameters for comparison among the different samples).

TABLE I
Characteristic Parameters in the Bi-Normal Distribution for the Thermally Bonded Nonwoven Filter Samples

Fiber	Fabric area density (g/m^2)	r_T (μm)	P_T (%)	r_S (μm)	r_L (μm)
PP/PET	45	40.3	96.2	35.7	57.0
	60	35.6	98.0	32.1	55.9
	80	32.8	91.6	28.5	43.8
	115	29.0	97.8	23.9	42.8
	140	25.2	93.2	20.9	31.8
	150	24.9	94.5	21.3	31.7
	175	24.6	95.9	20.2	32.7
	200	26.4	97.5	20.7	39.5
	215	26.7	97.0	20.0	37.5
PP/PET and PP	65	34.9	83.2	31.8	40.4
	83	34.2	94.9	31.6	46.8
	110	30.0	95.3	24.5	38.0
	122	23.6	71.4	21.3	26.2
	133	20.8	83.5	18.2	24.5
	150	21.4	79.6	19.5	23.8
	186	20.9	89.6	18.0	26.1
	215	18.3	86.0	15.3	20.7

parameters can completely determine the bi-normal distribution of the pore radius variations in the thermally bonded nonwoven samples.

Table I lists the characteristic parameters in the bi-normal distribution for the thermally bonded nonwoven filter samples with different fabric area densities. As a whole, all the r_T, r_S, and r_L decrease significantly to a certain value with increasing fabric area density, and then they become almost stable with further increase in the fabric area density. This is similar to the relationship between the air permeability and the fabric area density. Furthermore, with the addition of 10% PP fiber into the bi-component PP/PET fiber, all the r_T, r_S, and r_L of the different samples are reduced to some extent for an approximately identical fabric area density. This obviously leads to the decreased pore size and is in a good agreement with the effect of the constituent fibers on the pore size as shown in Figures 3 and 4.

Comparison with the commercial polyester filters

Commercial polyester filter bags of four performance levels, PE 1 p1s, PE 10 p1s, PE 50 p1s, and PE 100 p1s were obtained from a collaborating company. The different performance levels were produced to meet specific filtration requirements. The fabrics were needled and finished by singeing one side. Different denier fibers, such as 1.2, 3, 7, and 15 deniers, and different blending ratios were used to control the pore size. Figure 11 presents the SEM images taken from both the cross sections and surfaces of the PE 50 filter bag. Clearly, this fabric is much denser when compared with the thermally bonded nonwovens, as shown in Figure 2.

Table II lists the measured data of pore size, air permeability, and fabric area density for the commer-

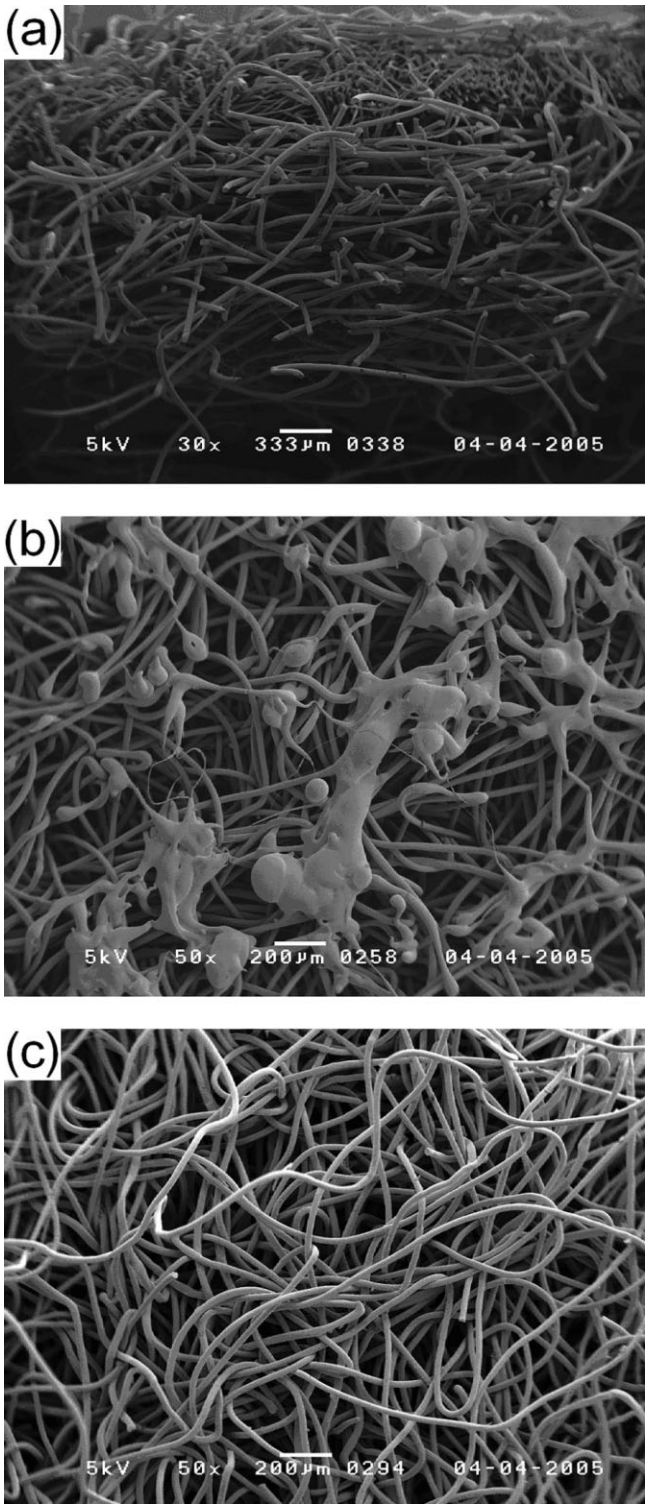

Figure 11 SEM images taken from (a) the cross section; (b) the singed surface; and (c) the other surface of the commercial filter bag PE 50.

TABLE II
Measured Data of Pore Size, Air Permeability, and Fabric Area Density for the Commercial Polyester Filter Bags

Sample code	Mean flow pore diameter (μm)	Bubble point pore diameter (μm)	Air permeability at 20 mm H_2O (L/min/cm^2)	Fabric area density (g/m^2)
PE 1 p1s	21.1	47.2	0.5	502.6
PE 10 p1s	40.1	78.5	1.3	391.9
PE 50 p1s	50.5	97.2	2.2	338.4
PE 100 p1s	60.9	112.0	2.4	452.7

cial filter bags. Table III lists the pore size, air permeability, and fabric area density for the thermally bonded nonwoven filter samples that are the most close to the specific filtration requirements of the corresponding commercial filter bags. Using only the bi-component PP/PET fiber, it is not possible to produce thermally bonded nonwoven filters that match both the bubble point pore diameter and the mean flow pore diameter of the commercial filter bag PE 1 p1s. However, it can achieve or closely near the corresponding pore diameter levels of the commercial filter bags PE 10 p1s, PE 50 p1s, and PE 100 p1. These pore diameter levels can be achieved by the thermally bonded nonwoven samples with higher air permeability and far lower fabric area densities.

Using the mixture of 90% PP/PET and 10% PP fibers can further reduce the fabric area density for achieving similar pore diameter levels and air permeability of the fabric from pure PP/PET bi-component fiber. To achieve both the bubble point pore diameter and the mean flow pore diameter of the commercial filter bag PE 1 p1s, a thermally bonded nonwoven filter with a fabric area density of 367.3 g/m^2 is required according to the data trend, but it is difficult to produce such a thermally bonded nonwoven filter because the air-laying web formation process has a maximum fabric area density of about 300 g/m^2. Heavier webs will block the air flow required for the fiber transportation. In the present work, the heaviest fabric area density for satisfying filter samples without appreciable process delay is 215 g/m^2 as listed in Tables I and III. However, by increasing the blend ratio of PP to PP/PET fibers, it is possible for the thermally bonded nonwoven filters to achieve both the bubble point pore diameter and the mean flow pore diameter of the commercial filter bag PE 1 p1s.

The thermally bonded nonwoven filter samples typically have higher air permeability, and hence lower pressure drop compared with those of the commercial filter bags. This can be attributed to the fact that structures of the former are not as dense as the latter, and one surface of the latter fabrics has been singed. It should be noted that noncontinuous fibers probably contribute to fiber shedding. Thus, prior to applications, the thermally bonded nonwoven filters may need to be singed on one side as well. This process has two effects. On the one hand, it decreases the pore size within the nonwoven fabrics. On the other hand, it may decrease the air permeability. However, as the air permeability values of the thermally bonded nonwoven filter samples are much higher than those of the commercial filter bags, the singeing process should not cause any problem with air permeability.

As aforementioned, pore size distribution is also associated with the flow properties of the filter media. Except for one irregular datum, the pore size variations in the commercial filter bags also follow all the bi-normal, bi-lognormal, and bi-Weibull distributions. Figure 12 represents the pore size distribution of the four performance levels of commercial filter bag me-

TABLE III
Pore Size, Air Permeability, and Fabric Area Density for the Thermally Bonded Nonwoven Filter Samples That Are the Most Close to the Specific Filtration Requirements of the Corresponding Commercial Filter Bags

Constituent fibers	Corresponding commercial filters	Mean flow pore diameter (μm)	Bubble point pore diameter (μm)	Air permeability at 20 mm H_2O (L/min/cm^2)	Fabric area density (g/m^2)
PP/PET	PE 1 p1s				
	PE 10 p1s	41.8	74.0	3.2	215
	PE 50 p1s	48.0	82.5	3.4	115
	PE 100 p1s	55.1	99.2	3.7	80
90% PP/PET and 10% PP	PE 1 p1s	33.6	51.9	1.1	215
	PE 10 p1s	38.7	60.8	1.3	186
	PE 50 p1s	47.0	80.9	3.4	83
	PE 100 p1s	49.1	102.1	3.7	65

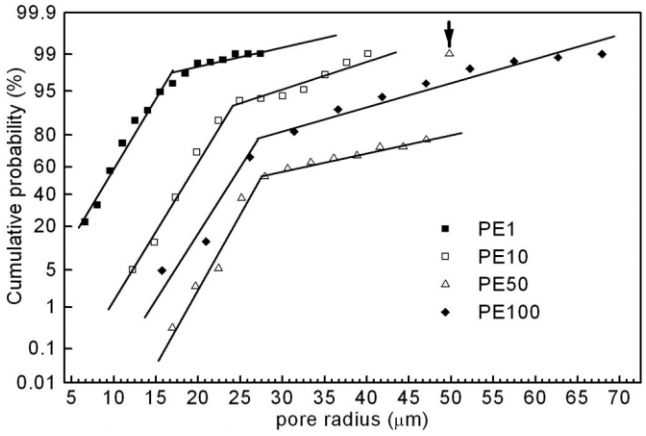

Figure 12 The cumulative probability curves of pore radius data series of the four types of commercial filter bags on normal probability coordinates (the solid arrow indicates the irregular datum).

dia on the normal probability coordinates. Table IV lists the characteristic parameters in the bi-normal distribution for the four performance levels of commercial filter bag media. Comparing Tables I and IV, it can be seen that except for the PE 1 p1s, the other three commercial filter bag media have either lower P_T or larger r_T than the corresponding thermally bonded filter samples as listed in Table III. In the terms of the pore size distributions, there are less relatively large pores in the latter samples than in the corresponding commercial filter bag media.

For a filter product, the pore structure, pore size distribution, air permeability, and fabric area density should all be taken into account. As such, the new 3D system can produce nonwoven filter bags as substitutes for most of the commercial polyester filter bag media. In addition, the thermally bonded nonwoven filters offer some advantages. First, because this method produces 3D products directly from fibers, the cost of the filter is much lower. Second, the thermally bonded filters have lower pressure drop, and thus require less energy to operate with the same fluid flow rate. In addition, the thermally bonded nonwoven filters normally have higher dust-holding capacity than filters made using other technologies due to their high porosity and dense gradient structure formed by the randomly orientated fibers. This translates into a longer filter life. All of these make the new 3D formation process very attractive for many filtration applications.

CONCLUSIONS

The thermally bonded nonwoven filter samples made from staple fibers have multiple filtration layers of interconnected pores and tortuous pore paths through the fabric thickness. The high porosity and a density gradient structure with interconnected pores in multiple filtration layers can obtain a slower increase in pressure drop with time and a larger dirt-holding capacity. This means longer filter life, fewer filter changeovers, and less downtime.

Both the bubble point pore diameter and the mean flow pore diameter of the thermally bonded nonwoven filter samples decrease nonlinearly, as the nonwoven fabric area density increases. This may be ascribed to the high porosity structure, interconnected pores, and tortuous pore paths through the fabric thickness. Furthermore, both the bubble point pore diameter and mean flow pore diameter increase linearly with increase in the reciprocal of the fabric area density. Compared with the nonwoven samples produced using only bi-component PP/PET fiber, the nonwoven samples produced using a mixture of 90% PP/PET and 10% PP fibers have smaller bubble point pore diameters and mean flow pore diameters due to their segmented bonding structure.

There is a significant linear relationship between both the bubble point pore diameter and the mean flow pore diameter and the air permeability. This shows that at the differential pressures used during the air permeability testing, both the bubble point pore diameter and the mean flow pore diameter can be used to characterize the air flow through the thermally bonded nonwoven fabrics.

The air permeability of the thermally bonded nonwoven filter samples decreases significantly to a certain value with increase in the fabric area density, and then becomes almost stable with further increase in the fabric area density. Such a result may be due to the effects of the high porosity structure and the interconnected pores and tortuous pore paths through the nonwoven fabric thickness. This is because of the density gradient structure, when the fabric area density increases slightly, for a lighter fabric area density, the additional layer is relatively denser and leads to a more significant decrease in the air permeability than that for a heavier fabric density, i.e., a thicker thickness.

The measured pore size data series in the thermally bonded nonwoven samples were found to follow all the bi-normal, bi-lognormal, and bi-Weibull distributions. Three characteristic parameters, the pore radius

TABLE IV
Characteristic Parameters in the Bi-Normal Distribution for the Four Performance Levels of Commercial Polyester Filter Bags

Sample code	r_T (μm)	P_T (%)	r_S (μm)	r_L (μm)
PE1	17.0	97.8	9.0	22.7
PE10	24.1	91.5	18.2	31.2
PE50*	27.8	52.3	25.0	44.2
PE100	27.2	77.7	23.0	36.9

at the intersect point of the two fitted lines, and the pore radii corresponding to the medians of the cumulative probability on the two fitted linear segments at the smaller and larger pore radii in the bi-normal distribution curves, exhibited similar dependence to that of the air permeability on the fabric area density. With the addition of 10% PP fiber into the bi-component PP/PET fiber, all the above three characteristic parameters of the different samples are reduced to some extent for an approximately identical fabric area density.

Taking the pore structure, pore size distribution, air permeability, and fabric area density into account together, the new 3D nonwovens system can produce thermally bonded nonwoven filter bags that can replace most of the commercial polyester filter bag media. The thermally bonded nonwoven filters can provide some additional advantages such as reduced product cost, lower energy costs, higher dust-holding capacity, and longer filter life.

References

1. Jena, A.; Gupta, K. Int Nonwoven J 2003, 12, 45.
2. Epps, H. H.; Leonas, K. K. Int Nonwoven J 2000, 9, 55.
3. Davis, N. C. Text Res J 1958, 28, 318.
4. Kothari, V. K.; Newton, A. J Text Inst 1974, 65, 525.
5. Atwal, M. S. Text Res J 1987, 57, 547.
6. Wang, X. Y.; Gong, R. H. J Appl Polym Sci, to appear.
7. Textiles–Determination of the permeability of fabrics to air; British Standards Institution: London, 1995. BS EN ISO 9237.
8. Textiles–Standard atmospheres for conditioning and testing; 1992 British Standards Institution: London, . BS EN 20139.
9. Walpole, R. E.; Myers, R. H. Probability and Statistics for Engineers and Scientists, 2nd ed.; Macmillan: New York, 1978.
10. Li, J. F.; Ding, C. X. Surf Coat Technol 2001, 135, 229.
11. Li, J. F.; Ding, C. X. J Mater Sci Lett 1999, 18, 1591.
12. Peterlik, H. J Mater Sci 1995, 30, 1972.
13. Bajpai, A. C.; Calus, I. M.; Fairley, J. A. Statistical Methods for Engineers and Scientists; John Wiley: Chichester, 1979.
14. Lin, C. K.; Berndt, C. C. J Mater Sci 1995, 30, 111.
15. Knalili, A.; Kromp, K. J Mater Sci 1991, 21, 6741.
16. Drape, M. R.; Smith, H. Applied Regression Analysis; Wiley: New York, 1981.
17. Li, T. Filtr Sep 1997, 34, 265.
18. Hassenboehler, C. B. Text Res J 1984, 54, 252.
19. Wehner, J. A.; Miller, B.; Rebenfeld, L. Text Res J 1987, 57, 247.
20. Sampson, W. W. J Mater Sci 2001, 36, 5131.
21. Dodson, C. T. J.; Sampson, W. W. J Pulp Pap Sci 1996, 22, J165.
22. Sampson, W. W. J Mater Sci 2003, 38, 1617.
23. Dodson, C. T. J.; Sampson, W. W. Appl Math Lett 1997, 10, 87.